FOCUSED REVIEW SERIES: Photodynamic Therapy
Print ISSN 2234-2400 / On-line ISSN 2234-2443
Clin Endosc 2013;46:7-23
http://dx.doi.org/10.5946/ce.2013.46.1.7

Open Access

Advance in Photosensitizers and Light Delivery for Photodynamic Therapy

Il Yoon, Jia Zhu Li and Young Key Shim

PDT Research Institute, Inje University School of Nano System Engineering, Gimhae, Korea

The brief history of photodynamic therapy (PDT) research has been focused on photosensitizers (PSs) and light delivery was introduced recently. The appropriate PSs were developed from the first generation PS Photofrin (QLT) to the second (chlorins or bacteriochlorins derivatives) and third (conjugated PSs on carrier) generations PSs to overcome undesired disadvantages, and to increase selective tumor accumulation and excellent targeting. For the synthesis of new chlorin PSs chlorophyll a is isolated from natural plants or algae, and converted to methyl pheophorbide a (MPa) as an important starting material for further synthesis. MPa has various active functional groups easily modified for the preparation of different kinds of PSs, such as methyl pyropheophorbide a, purpurin-18, purpurinimide, and chlorin e6 derivatives. Combination therapy, such as chemotherapy and photothermal therapy with PDT, is shortly described here. Advanced light delivery system is shown to establish successful clinical applications of PDT. Phtodynamic efficiency of the PSs with light delivery was investigated *in vitro* and/or *in vivo*.

Key Words: Photochemotherapy; Photosensitizing agents; Chlorophyll and chlorins; Photothermal therapy; Light delivery

INTRODUCTION

Photodynamic therapy (PDT) is a promising non-invasive anticancer therapy and is still under investigation.[1] As a feasible binary cancer therapy matured at several institutions throughout the world in the 1980's, PDT consists of the administration and selective accumulation of a photosensitizer (PS) in target tumor tissues, followed by generation of singlet oxygen ($^1O_2$) and other cytotoxic reactive oxygen species (ROSs) that result in cell membrane damage and subsequent cell death upon irradiation with light of appropriate wavelength in the presence of tissue oxygen.[2,3]

PDT is the most important biomedical application of photodynamic action. Although the therapeutic properties of light for the treatment of various diseases in dermatology were known in ancient civilizations, the importance of the light treatment for cutaneous diseases started to be recognized at the beginning of the last century when Niels Finsen received the Nobel Prize in this field. The concept of photodynamic action also dates back to when Oscar Raab from Tappeiner group used eosin together with light to treat skin cancer.[4]

The modern explosion of interest in PDT began with the discovery and study of hematoporphyrin derivative (HpD) by Lipson and Schwartz at the Mayo Clinic in 1960,[5] and accelerated by pioneering studies in both basic science and clinical application by Dougherty et al.[6] In 1983, a partially purified form of HpD, now commercially known as Photofrin (porfimer sodium; QLT, Vancouver, BC, Canada), was developed. Photofrin was the first PS to receive regulatory approval for treatment of various cancers in more than 40 countries throughout the world, including the United States (by Food and Drug Administration [FDA] in 1995).

Although the first generation PS Photofrin has been shown to be efficacious in the treatment of many cancer types, it has some disadvantages, including suboptimal tumor selectivity,[7] low absorption of light and poor light penetration into the tumor due to the relatively short wavelength absorption (630 nm),[8] prolonged skin photosensitivity of patient,[9] and the fact that it was a complex mixture of uncertain structure.[10] Therefore, to overcome these drawbacks and improve the treatment

Received: November 21, 2012 **Revised:** December 14, 2012
Accepted: December 14, 2012

Correspondence: Young Key Shim
PDT Research Institute, Inje University School of Nano System Engineering, 197 Inje-ro, Gimhae 621-749, Korea
Tel: +82-55-320-3871, **Fax:** +82-55-336-3872, **E-mail:** ykshim@inje.ac.kr

efficacy, several strategies have been employed for the development of more tumor-selective agents with reduced side effects, especially skin phototoxicity. Some second generation PSs have recently been developed and were introduced in clinical trials. Most of them are cyclic tetrapyrroles, comprising substituted derivatives of porphyrin, chlorin, and bacteriochlorin. Examples of these PSs are shown in Fig. 1, including Tookad (palladium bacteriopheophorbide; MedKoo Biosciences, Chapel Hill, NC, USA; Fig 1A), Antrin (Lu texaphyrin, a tripyrrole expanded macrocycle; Pharmacyclics Inc., Sunnyvale, CA, USA; Fig. 1B), benzoporphyrin derivative monocarboxylic acid (BPD-MA; Fig. 1C), Purlytin (Tin ethyl etiopurpurin; Miravant Medical Technologies, Santa barbara, CA, USA; Fig. 1D), Foscan (meso-tetrahydroxyphenyl chlorine; Biolitec Pharma Ltd., Dublin, Ireland; Fig. 1E), and zinc (II) phthalocyanine (Pc; Fig. 1F), all of which have strong absorption at 650 to -750 nm.[11]

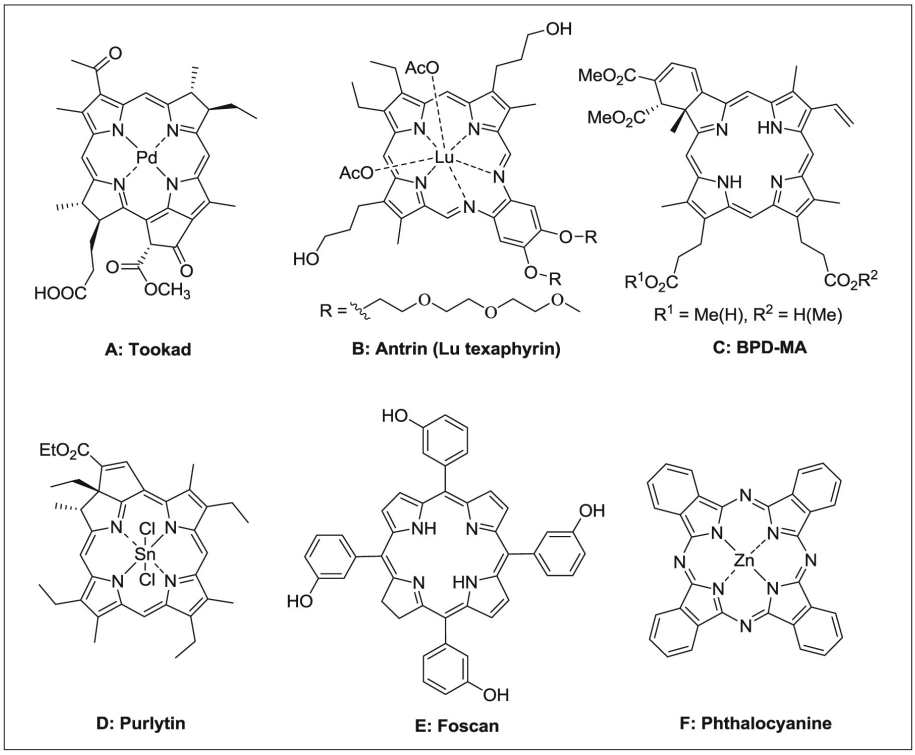

Fig. 1. Examples of second generation photosensitizer. (A) Tookad. (B) Antrin (Lu texaphyrin). (C) Benzoporphyrin derivative monocarboxylic acid (BPD-MA). (D) Purlytin. (E) Foscan. (F) Phthalocyanine.

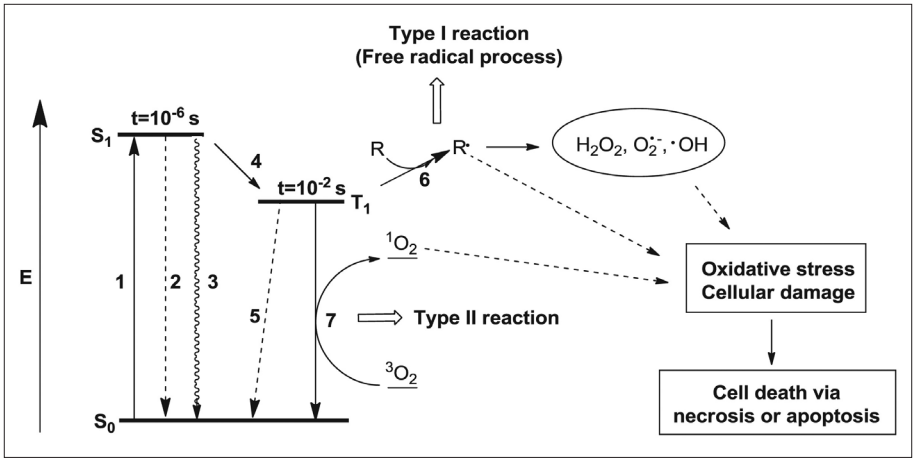

Fig. 2. Modified Jablonski diagram. Photophysical processes involved in photodynamic therapy: 1) absorption, 2) fluorescence, 3) internal conversion, 4) intersystem crossing, 5) phosphorescence, 6) formation of free radicals by energy transfer from T_1 photosensitizer to biological substrates, and 7) formation of singlet oxygen ($^1O_2$) by energy transfer from T_1 photosensitizer to triplet oxygen ($^3O_2$). Adapted from Sternberg et al. Tetrahedron 1998;54:4151-4202, with permission from David Dolphin.[12]

Basic principles of PDT

The photophysical processes involved in PDT are illustrated in Fig. 2.[12] 1) The PS is activated from its singlet ground state (S_0) to the short-lived first excited singlet-state (S_1) upon absorption of light with appropriate wavelengths. 2) The S_1 PS can return to the S_0-state by emitting the absorbed energy as fluorescence or 3) by internal conversion. 4) Alternatively, it can also convert to the relatively long-lived first excited triplet state (T_1) by intersystem crossing. 5) The T_1 PS can return to the S_0-state by emitting phosphorescence. However, energy transfer from T_1 to biological substrates or molecular oxygen generates ROSs ($^1O_2$, H_2O_2, $O_2^{\bullet -}$, •OH), which produce cellular damage to death mainly by necrosis or apoptosis method.

There are two proposed types of photochemical pathways, known as type I and type II reactions.[13] In the type I reaction, the PS interacts with a biomolecule (or oxygen) resulting in hydrogen atom (or electron) transfer that leads to the production of free radicals. In the type II reaction, singlet oxygen is generated as a result of energy transfer from the T_1 PS to the triplet ground state of molecular oxygen. It is suggested that parallel to the type I and type II mechanisms, there might proceed a direct interaction between the relatively long-lived triplet sensitizer and free radicals present in the system, a so called triplet-doublet process, which have been known as the modified type I (MTO) mechanism.[14] Experimental results and further kinetic approach since then made it clear that this MTO mechanism differs basically from the type I and thus be called the type III mechanism.[15,16] Although these three pathways could be occurred in the photosensitization process, however, it is suggested that the type II predominates over the others, in that singlet oxygen shows relatively high reactive property and causes irreversible destruction of tumor cells.[3]

Mechanism of the selective tumor localization of PS

The phenomenon that porphyrins and their derivatives can localize in tumor tissues has been intensively studied since the first observations[17] and progress have been made;[18] the mechanisms involved, however, are still not completely understood. Boyle and Dolphin[19] reported tumor normal tissue ratios from many experimental studies of PSs in animal models. The mechanism is very complex in that there were large variations even with the same PS when comparing different PS structures, different tumor models, during or after the injection, and doses.

The PSs with different pharmacokinetics seem to have different tumor localization ability,[20] and this ability of the PS with the faster pharmacokinetics is probably due to selective accumulation in the tumor because of the increased permeability in tumor neovasculature.[21] While the localization of PS with slower acting pharmacokinetics is more likely due to selective retention, which was suggested to be caused by some distinctive properties of tumor cells compared to normal tissue, such as the relatively low pH value,[22] the overexpressed low density lipoprotein (LDL; apoB/E) receptor,[23] poorly developed lymphatic drainage,[24] and some tumor-associated macrophages.[18,25] It has also been suggested that the porphyrin based PS can be accumulated in mitochondria via the peripheral benzodiazepine receptors located on the inner mitochondrial membrane.[26]

"Phototherapeutic window" in PDT

The most coherent light sources for PDT are lasers. Penetration of light through tumor tissue is highly complex in that light is either scattered or absorbed when it enters tissue, and the extent of both processes depends on tissue type and light wavelength. The light absorption characteristics of tissues decrease with increasing wavelength, hence longer wavelengths of light penetrate more efficiently through tissue. The combination of absorption of lower wavelength light by the important endogenous chromophores (reduced form of nicotinamide adenine dinucleotide [NADH], collagen, lipopigments, deoxyhemoglobin, flavins, and melanin) together with reduced light scattering at longer wavelengths and the occurrence of water absorption at wavelengths greater than 1,300 nm has led to the concept of the "optical window" in tissue.[11,27]

In PDT, shorter wavelengths (<650 nm) have less tissue penetration and are mostly absorbed, resulting in high skin photosensitivity. Otherwise, absorption bands at longer wavelengths (>850 nm) are not sufficient for the PS triplet state to transfer from the ground state oxygen molecule to generate excited singlet oxygen. Therefor the maximum of tissue permeability occurs within the range of approximately 650 to 850 nm. Such range, called the "phototherapeutic window," is predominantly used in PDT.[28] Hence, PS should preferably have strong electronic transition intensities in this phototherapeutic window, where light penetration into the animal tissue is maximized.

Classification and characteristics of the ideal PSs

PSs are generally classified as the first, second and third generations.[29] The first generation PSs include HpD and Photofrin. The second generation PSs has been developed since the late 1980s to overcome the disadvantages of the first generation PSs. The third generation PSs are referred to those second generation PS conjugates coupled on carriers such as cholesterol, antibodies, and liposomes for selective accumulation and targeting within tumor tissue.[30]

In searching for new and better PSs, the following characteristics have been generally accepted as criteria for ideal PSs;[11,29-31] 1) It should be chemically pure and of known speci-

fic composition that is stable at room temperature and with a straightforward synthesis; 2) It should possess minimal dark toxicity and only be cytotoxic in the presence of light at defined wavelength; 3) It should have preferential retention by target tissue (tumor cells), and should be rapidly excreted from the body, thus inducing a low systemic toxicity; 4) It should have strong absorption with high extinction coefficient (ε) at longer wavelength (between 700 to 800 nm) where scattering of light is minimal and tissue penetration is maximum; 5) It should have excellent photochemical reactivity, with high triplet state yields and long triplet state life times and be able to effectively produce singlet oxygen and other ROSs; and 6) Finally, it should be inexpensive and commercially available in order to promote extensive utilization of the treatment, and should be easy to dissolve in the body's tissue fluids and should be capable of formulation.

PDT

Chlorophyll (Chl) PS

The photo-inactivition of tumors by Hp mixtures led to the various second generation PSs that have been developed to improve PDT. Most of them are cyclic tetrapyrroles, comprising substituted derivatives of porphyrin, chlorin, and bacteriochlorin (Fig. 3). PS can easily be prepared by partial syntheses starting from abundant natural starting materials, such as heme, Chl, and bacteriochlorophyll, which attracted maximum interests in that they have both economic and environmental advantages compared to those prepared by complicated total chemical synthesis.[11,31]

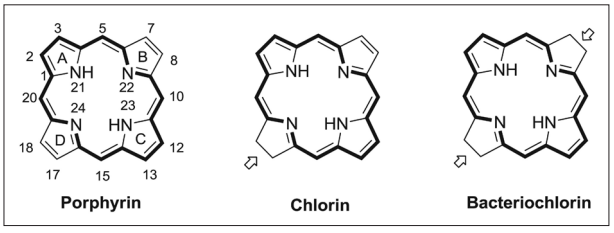

Fig. 3. Comparative structures of porphyrin, chlorine, and bacteriochlorin. The bold lines indicate the 18π electron [18]-diazaannulene aromatic pathway.

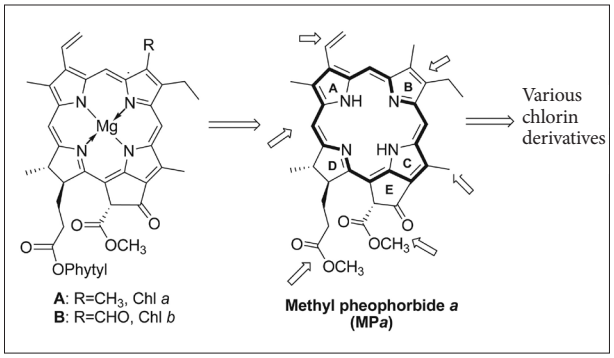

Fig. 4. The structures of Chl a and b, and methyl pheophorbide a (MPa).

Naturally occurring Chls substituted chlorin derivatives. Chl a and Chl b (Fig. 4) occur in all green plants and are the most common natural Chls, in which the longest wavelength absorption band shifts to 650 to 690 nm range and increases several fold in height, the factors highly desirable to PS. Additional advantage of using Chl a is an economic isolation in large amounts from plants or algae. Smith developed an effective measure to prepare Chl a by starting from *spirulina* algae which contain only Chl a (no Chl b).[32] *Spirulina* algae is also commercially available in the form of freeze-dried powder.

The second generation PSs

Chl a is not suitable for using in PDT due to its high aggregation tendency and low solubility in physiological liquids, but may provide a suitable source for the synthesis of new PSs that comply with the pharmaceutical requirements.[31] Fig. 5 shows some second generation Chl PSs used in PDT for preclinical and clinical studies. Bellnier et al.[33] and Pandey et al.[34] synthesized and evaluated a series of amphiphilic alkyl ether ana-

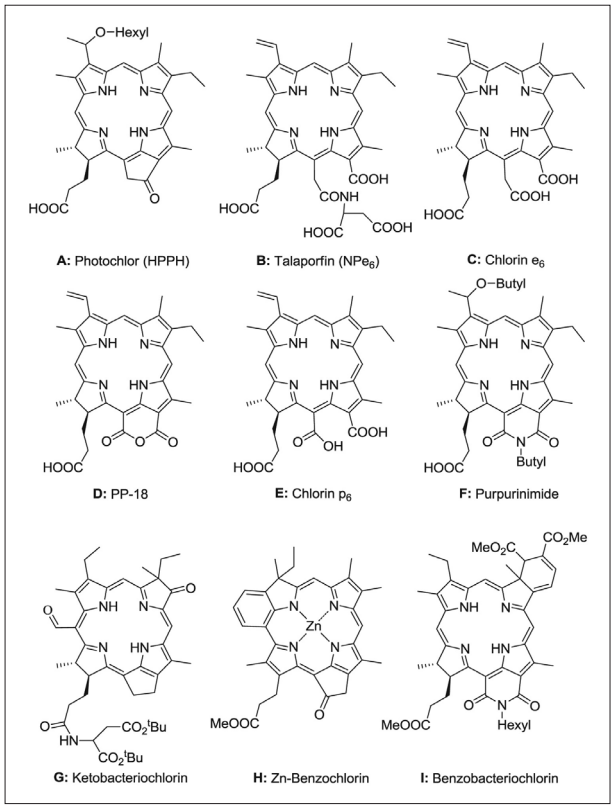

Fig. 5. Structures of some Chl derivatives as photosensitizers in photodynamic therapy. (A) Photochlor (2-[1-hexyloxyethyl]-2-devinyl pyropheophorbide-a, HPPH). (B) Taraporfin (Mono-L-aspartyl chlorin e6, NPe6). (C) Chlorin e6. (D) Purpurin (PP)-18. (E) Chlorin p6. (F) Purpurinimide. (G) Ketobacteriochlorin. (H) Zn-Benzochlorin. (I) Benzbaceriochlorin.

logs of pyropheophorbide a, in which the hydrophobicity increases with the length of the alkoxy group at the 3^1-position. It was found that the hexyl ether derivative (2-[1-hexyloxyethyl]-2-devinyl pyropheophorbide-a, HPPH) is the most effective among the compounds evaluated (Fig. 5A). The PDT properties of HPPH have been studied extensively *in vitro* and *in vivo*, and it is regarded as a promising PS candidate for PDT in that, compared to the first generation PS, HPPH shows improved pharmacokinetic properties and causes only mild skin photosensitivity which declines rapidly within a few days after administration.[35] It is also known as Photochlor (Medkoo Biosciences), and was approved in the USA to treat cancer in phase I/II clinical trials.[36,37]

Mono-L-aspartyl chlorin e6 (NPe6) is a chemically pure hydrophilic chlorin PS derived from Chl a with good photosensitization ability (exhibits significant absorption at 664 nm and has a molar extinction coefficient of 4×10^4 $M^{-1}cm^{-1}$) (Fig. 5B). The hydrophilic character is mainly due to the presence of four ionizable carboxyl groups, which are located on the same side of the macrocycle. The amphiphilic character of NPe6 is also helpful for using in PDT.[38] Another important advantage of NPe6 is its fast kinetics; the clearance time in mouse has been found to be 30.3 hours so it does not cause prolonged photosensitivity after PDT.[39] However, its synthetic matrix chlorin e6 (Fig. 5C) has been found to be photocytotoxic, which is why there has not been much research on it as a candidate PS for PDT.[40] NPe6 was approved in Japan for the treatment of early centrally located lung cancer, and pPhase III clinical trials on using NPe6 for the treatment of hepatocellular carcinoma is also undergoing.[29,41,42]

Having a 6-membered anhydride ring, purpurin-18 (PP-18) (Fig. 5D) is easily prepared from pheophorbide a and its esters as a result of oxidative cleavage of isocyclic ring E.[43] PP-18 is lipophilic, has a strong absorption at 700 nm and a good singlet oxygen quantum yield (about 0.7);[44] however, it is not a suitable PS due to the instability of the anhydride ring *in vivo*.[45] The water-soluble chlorin p_6 (Fig. 5E), obtained by alkaline cleavage of the anhydride ring of PP-18, absorbs at 656 nm and provides singlet oxygen quantum yield of about 0.6 in ethanol, the same as chlorin e6.[44] Chorin p_6 has been found to be phototoxic,[43] but it has not been studied much for use in PDT, whereas its 13^1-lysylamide methyl ester has sometimes been used in PDT research.[46]

Purpurinimide (PPI) analogs derived from PP-18 have an added advantage when compared with other chlorins in that they exhibit advantageous light absorption characteristics in the red region of the spectrum (706 to 718 nm).[47] Following a similar quantitative structure activity relationship-investigation approach with HPPH, a series of lipophilic PPI derivatives with various alkyl and fluoroaryl substitutions at the C-3, C-8, C-12, C-20, and N-13 positions of the macrocycle were synthesized and their photodynamic efficacies were evaluated *in vivo*. The long wavelength absorption of those compounds was near 700 nm and they had singlet oxygen quantum yield of 0.57 to 0.60.[48] It was found that the location of alkylether substituents in those compounds was important for their photosensitizing efficiency. Among those PPI analogs, the 3^1-O-butyl-13^2-N-butyl PPI shows the best photosensitizing efficiency as well as tumor uptake (12.90 μmol/kg), making it a promising potential Chl PS (Fig. 5F).[49]

A series of ketobacteriochlorins developed by Pandey group exhibit long wavelength absorptions in 750 to 800 nm range, and have singlet oxygen quantum yield near 0.40.[50] *In vivo* PDT efficacies of these ketobacteriochlorins were also evaluated. It was found that aspartic acid ditetrabutyl ester coupled with ketobacteriochlorin (Fig. 5G) tends to clear rapidly from the tumors and shows the best photosensitizing efficiency at the drug dose of only 1.0 mg/kg and the light dose of 135 J/cm after 3 hours but not 24 hours post injection.[50]

Other strategies for developing new Chl PSs include the formation of benzochlorins and benzobacteriochlorins, which can influence deeply on their electronic absorption properties. Benzochlorin zinc complex (Fig. 5H) developed by Pandey et al.[47] and Mettath et al.[51] has absorption maxima at 759 nm, and was found to be toxic at higher drug doses (5.0 mmol/kg) after exposing the tumor with light, but no significant long-term tumor cure was observed at lower drug doses. On the other hand, benzobacteriochlorins formed by Diels-Alder reaction of 8-vinyl chlorin derivative with various dienophiles show their absorption maxima in 737 to 805 nm range. The *in vivo* efficacy of these long wavelength benzobacteriochlorins was determined in C3H mice transplanted with radiation-induced fibrosarcoma tumors, which found that, among all bacteriochlorins, the N-hexyl-substituted benzobacteriochlorin (Fig. 5I) was most effective, producing 40% tumor response at the drug dose of 5.0 μmol/kg and the light dose of 135 J/cm at 24 hours post injection at the appropriate long wavelength absorption.[52]

The third generation PSs

A further generation of PSs represents an emerging class worth addressing and an active research area in the field. Certain second generation PSs have been conjugated to carrier molecules that deliver PSs specifically to tumor tissue. These carrier molecules include monosaccharide,[53] peptides,[54] LDLs,[55] antibodies,[56] polymeric nanoparticles (NPs)[57] and polymers.[58] Chl derivatives possess various functional groups to which conjugation is possible by multifarious synthetic strategies, therefore exhibit the advantages in developing the improved PDT agents.[47]

For efficacious targeting PS to tumor cells, it is necessary to take advantage of certain properties of the tumor cells that differentiate them from normal cells. In an effort to enhance the efficacy and selectivity of PSs, Zheng and Pandey groups have developed conjugates of pyropheophorbide,[59] PPI,[60] and HPPH[61] with different numbers of saccharides. It is hoped that these conjugates would target carbohydrate-binding molecules, such as the carbohydrate binding lectins galectin-1 and -3, which are known to be differentially expressed on the surface of many tumor cells.[53,62] Zhang et al.[59] demonstrated that the PS pyropheophorbide 2-deoxyglucosamide (Fig. 6A) selectively accumulated in the tumors. From the comparative *in vitro*/*in vivo* studies of a series of the positional isomers of lactose-PPI conjugates, it was found that carbohydrate conjugates showed higher binding affinity than the corresponding nonconjugated PPIs, and the PDT efficacy showed a remarkable difference depending on the position of the carbohydrate moiety. Among these conjugates, the conjugate containing a lactose moiety at three-position of the PPI system (Fig. 6B) was found to be most effective.[60] From the study on HPPH with different numbers of saccharides conjugated,[61] it was noted that carbohydrate conjugates and unconjugated HPPH had similar singlet oxygen yields but showed different intracellular localization. Among the resulting carbohydrate conjugates, HPPH-Gal (Fig. 6C) exhibited increased antitumor activity over that of HPPH. This could not be explained by enhanced PS binding to cellular galectins.

Peptides can also be used to enhance the tumor cellular uptake of PS-carrier conjugates. In order to target cancer cells overexpressing the folate receptor, Stefflova et al.[63] conjugated folate to pyropheophorbide a with or without a peptide linker and studied their accumulation in mice bearing overexpressing or nonexpressing folate receptor cancer cells, respectively. It was found that the conjugate with the peptide linker, compared to that without the peptide linker, tended to specifically accumulate into the folate receptor overexpressing tumor cells in contrast to kidneys and liver. Another approach used by Chen et al.[64] conjugated pyropheophorbide a and a $^1O_2$ scavenger (carotenoid) together by a specific target peptide which is specific to a caspase-3 protease that is expressed in the cancer cells. This conjugate can efficiently inhibit $^1O_2$ generation thereby minimize photo damage to nontarget cells, whereas in the presence of a targeted protease, the peptide linker is cleaved and the PS and quencher will separate so that the PS can be photo activated. A chlorin e6-poly-L-lysine conjugate has been reported to exhibit nuclear localization in HeLa cells resulting in enhanced PDT efficacy. The cellular uptake of this conjugate for HeLa cells was much higher than that of chlorin e6. It was found that such conjugate was accumulated in the nucleus of HeLa cells.[65] In another study, a nuclear localization sequences (NLS) peptide was introduced on a polymer-PS conjugate, which conjugated mesochlorin e6 mono-ethylene diamine (Mce6) with *N*-(2-hydroxypropyl) methacrylamide (HPMA).[66] It was demonstrated that a cationic NLS peptide enhanced the PDT efficiency compared to a non-NLS containing conjugate by targeting the nucleus.

Similarly to saccharides and peptides, proteins can be conjugated to PS to increase cancer cell specificity targeting specific subcellular compartments. Conjugation of PS with the Shiga-like toxin B subunit to target the cell surface glycosphingolipid receptor Gb_3, overexpressed in ovarian carcinomas and Burkitt's lymphomas,[67] has been applied to chlorin e6, which resulted in enhanced photodynamic destruction of cancer cells *in vitro* by factor of 10 compared to chlorin e6.[68]

To target LDL receptors (LDLr) that is overexpressed in the tumor cells, a pyropheophorbide cholesterol oleate conjugate which serves as a double anchor for the LDL lipid core was synthesized and successfully reconstituted into the LDL lipid core. Laser scanning confocal microscopy studies demonstrated that this PS-reconstituted LDL can be internalized via LDLr by human hepatoblastoma G_2 tumor cells and, therefore, can be used as a PDT agent directed at LDLr overexpressing tumors.[69] In a recent study, chlorin e6-cholesterol conjugate and its copper complex were prepared and studied for their entrapping properties in phospholipid vesicles. The resulting conjugates are supposed to have affinity to membranes, and may be used as PSs, being entrapped in liposomes.[70]

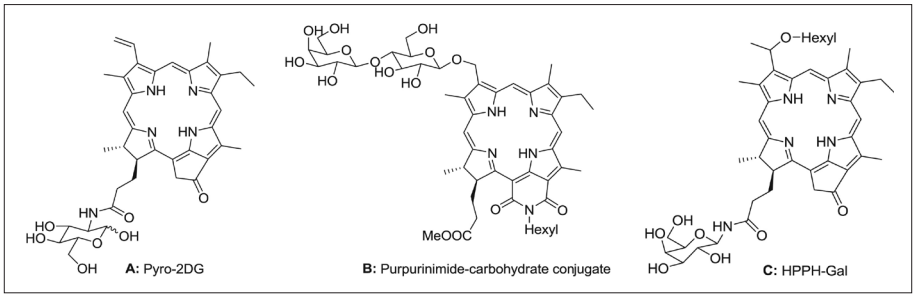

Fig. 6. Structures of photosensitizer-carbohydrate conjugates. (A) Pyropheophorbide 2-deoxyglucosamide (Pyro-2DG). (B) Purpurinimide-carbohydrate conjugate. (C) A 2-(1-hexyloxyethyl)-2-devinyl pyropheophorbide-a (HPPH)-Gal.

Interest in NPs as PS carriers has been increasing in recent years. A novel ceramic-based NPs entrapping water-insoluble HPPH was recently reported.[71] It can provide stable aqueous dispersion of HPPH, yet preserve the key step of the necessary photo generation of singlet oxygen. Covalent bonding of the HPPH into organically modified silica NPs creates more stable formulations.[72] It was reported that the NPs (about 20 nm in diameter) retained their spectroscopic and functional properties and could robustly generate cytotoxic singlet oxygen molecules upon photo irradiation. It was also demonstrated that these NPs are avidly uptaken by tumor cells *in vitro* with subsequent phototoxic action. The same group described a stable multifunctional polymeric micelle-based nano carrier system which encapsulated HPPH and magnetic Fe_3O_4 NPs.[73] The micelles were efficiently taken up by cells and its phototoxicity was retained, and these NPs had a role in magnetically directed delivery to tumor cells and enhanced imaging.[73]

Synthesis

Chemical modification of Chl a

The chemistry of Chls is dominated by the aromatic character of the basic tetrapyrrole moiety and the reactivity of the functional groups in the side chains (Fig. 4). As a cyclic tetrapyrrole with a fused five-membered ring, the overall reactivity of Chls is similar to a standard heteroaromatic compound.[74] There are various active functional groups surrounding Chl a basic macrocycle, such as 3-vinyl, β-keto ester in the isoylic ring E, and 17-ester group, which can be modified without destroying its aromatic character to obtain many different types of stable chlorin derivatives, such as methyl pheophorbide a (MPa),[75] methyl pyropheophorbide a,[76] methyl pyropheophorbide d (MPPd),[77] PP-18,[78] PPI,[79] chlorin e6,[80] chlorin p_6,[44] etc.

MPa derived from Chl a was used as a starting material to synthesize a series of stable chlorin derivatives having reactive groups, which laid the foundation of further linkage with some biologically active groups.

Preparation of MPa from Chl paste

Instead of alga *spirulina maxima*, Chl paste (an extract from *excrementum bombycis*, the main composition of which are Chl a and Chl b, obtained from Shandong Guangtongbao Pharmaceuticals Co., Ltd., Qingzhou, China) was used as the starting material to prepare MPa, 1, one of the most widely used Chl derivative which can be converted into many kinds of chlorin derivatives such as methyl pyropheophorbide a (MPPa, 2), PP-18 methyl ester 4 and chlorin e6 derivatives by simple strategies (Fig. 7). Following the reported method[75] with minor modifications, Chl paste was dissolved in 5% H_2SO_4 in methanol, and stirred at room temperature under nitrogen for 12 hours, followed by filtration, extraction, concentration, and separation on silica gel column to obtain MPa 1 (5.1%) with relatively high yield compare to the reported method using alga *spirulina maxima* as the starting material (Fig. 8).[75]

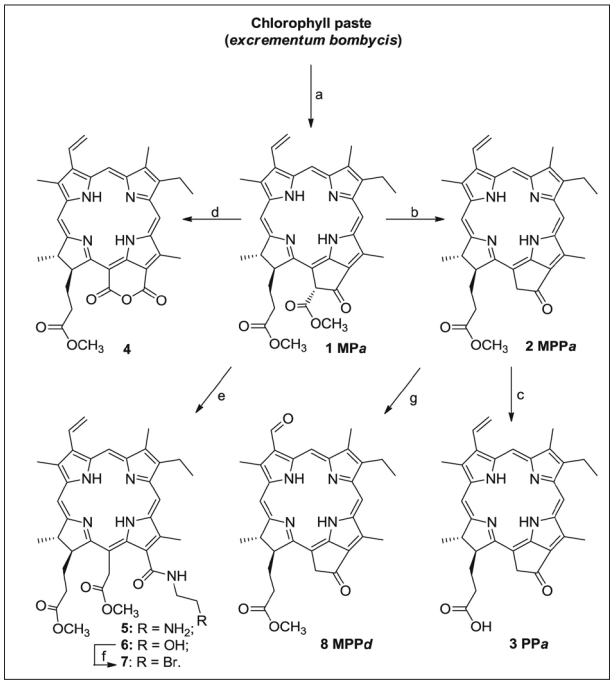

Fig. 7. Synthesis of the basic chlorin derivatives having reactive groups. Reaction conditions: a) 5% H_2SO_4 in MeOH, N_2, 12 hours. b) 2, 4, 6-collidine, N_2, reflux, 2 hours; c) aq. LiOH, N_2, 1.5 hours; d) KOH/1-propanol/pyridine/air, 2 hours; CH_2N_2; e) $H_2NCH_2CH_2R$, CH_2Cl_2, 2 hours; f) CBr_4, PPh_3; g) OsO_4, $NaIO_4$, 6 hours. MP, methyl pheophorbide; MPP, methyl pyropheophorbide; PP, purpurin.

Synthesis of chlorin derivatives with various active functional groups from MPa

It is well known that MPa 1 is the key intermediate in the multitude of derivatizations of Chl a. Chlorin derivatives with various reactive groups such as carboxyl (3, 17), formyl (8), amino (5, 11, 13, 14), hydroxyl (6, 9, 15), and bromo (7, 18) groups were synthesized using MPa 1 as the starting material (Figs. 7, 8).

As shown in Fig. 7, following the reported methods, MPPa 2 was obtained by refluxing the MPa 1 in 2, 4, 6-collidine under N_2 atmosphere for 2 hours,[76] and aqueous LiOH was used under N_2 to hydrolyze the 17-methyl ester group of MPPa 2 to give pyropheophorbide a 3 which have a free carboxylic group.[81] By air oxidization in base condition, and followed by methylation using diazomethane, MPa 1 was converted into PP-18 methyl ester 4.[78] Chlorin e6 amide derivatives 5 and 6 which have free hydroxyl and amino group, respectively, were synthesized in good yield using the reaction of nucleophilic substitution at C-13[1] in the isocyclic ring E of MPa 1. In gener-

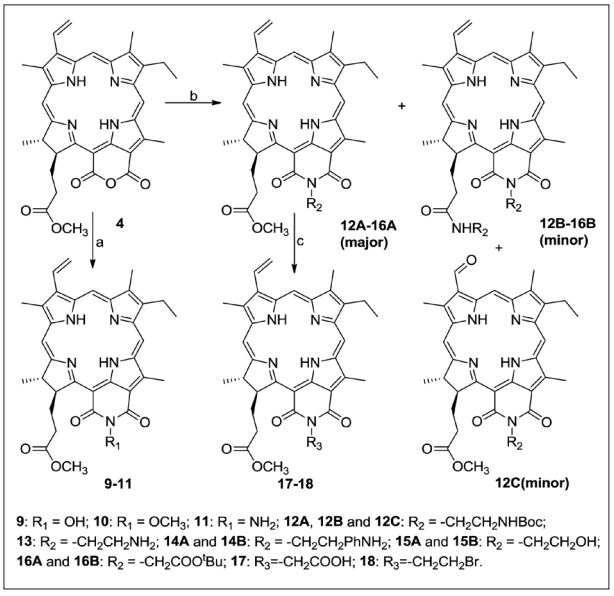

Fig. 8. Synthesis of purpurinimides having active groups. Reaction conditions: a) RNH_2, pyridine, 5 hours; b) RNH_2, Toluene, N_2, reflux, 6 to 12 hours, c) from 16A to 17, TFA; from 15A to 18, CBr_4, PPh_3. MP, methyl pheophorbide; MDD, methy pyropheophorbide; PP, purpurin.

al, MPa 1 and amine (e.g., 2-aminoethanol) were stirred in dichloromethane at room temperature for several hours to give the corresponding chlorin e6 amide derivatives. Hydroxyl group of compound 6 was transformed to bromo group by nucleophilic substitution using carbon tetrabromide and triphenyl phosphine as reagents to give compound 7. MPPd, 8 was obtained by oxidizing the 3-vinyl of MPPa 2 with OsO_4/$NaIO_4$.

PP-18 methyl ester 4, as shown in Fig. 8, was transformed to PPI derivatives 9-16 with reactive groups via two pathways. In the first approach, PP-18 methyl ester 4 and active amines (e.g., hydroxylamine hydrochloride) were stirred in pyridine for several hours to give PP-18-*N*-hydroxylimide methyl ester 9 and PP-18-*N*-aminoimide methyl ester 11 in high yield, respectively. Methylation of compound 9 by diazomethane led to the production of PP-18-*N*-methoxyl imide methyl ester 10. In the second approach, PP-18 methyl ester 4 and amines were refluxed in toluene under nitrogen for 6 to 12 hours to give the corresponding PPI 12A-16A in moderate yield, and the related amide analogues 12B-16B (in which the methoxycarbonyl functionality [CO_2Me] of 17-propionic ester [$CH_2CH_2CO_2Me$] was replaced with amide [-CONHR]) as minor products, and another by product 12C having 3-formyl group was also found during refluxing PP-18 methyl ester 4 and *N*-Boc-ethylenediamine in toluene. Compound 17 was obtained from 16A by deprotection of tetrabutyl ester in the presence of TFA. Compound 18 was obtained from compound 15A by transforming its hydroxyl group to bromo group using carbon tetrabromide and triphenyl phosphine as nucleophilic reagents.

Characterization of chlorin derivatives prepared from Chl a

The most important feature of the chlorins derived from Chl is the large π-system of the macrocycle which produces an "induced ring current," which causes peripheral protons in the plane of the macrocycle (*meso*-H, 3-vinyl, 2, 7, 12-CH_3, 8^1-CH_2, and 13^2-CH_2) to be deshielded, making the shifts of which appear downfield of their corresponding groups. Otherwise, protons situated above or below the plane of the macrocycle (8^2-CH_3, 17-propionic side chain, 18-CH_3, and 8^2-CH_3) are significantly shielded, making the shifts of which appear upfield of their corresponding groups, and the central NH protons are strongly shielded and appear upfield of tetramethyl silane. This ring current effect accounts for the large range of chemical shift values (about 10 ppm) seen for Chl derivatives (MPPa 2).

The absorption spectrum is simple, most useful and extensively used analytical property to characterize phorphyrin and chlorin and requires only 10 μg or less. Absorption spectra of chlorins show the electronic transitions along the X axis of the chlorin running through the nitrogen (N) atoms of rings B and D, and along the Y axis through the N atoms of rings A and C. The two pairs of absorption bands in the blue and red spectral regions in chlorins are called B (or Soret) and Q bands, respectively, and arise from π-π* transitions of the four frontier orbitals.[82] One band of each pair is polarized along the X axis (B_x, Q_x), the other along the Y axis (B_x, Q_y). The polarizations of the transitions along the axes are called X and Y. In MPPa (2), for example, the spectrum is characterized by two strong overlapping Soret (B) bands at about 410 nm and a relatively strong Q_y band at 668 nm with weak Q_x bands at 500 to 600 nm range.

Q_y band takes an important role for chlorins used as PS in PDT. Chlorins used in this study show various Q_y absorption bands at 660 to 708 nm range due to the different peripheral substituents situated along the Y axis, especially the change of isocyclic ring E. MPPa (2) which has a fused isocyclic 5-memberd ring E shows its Q_y absorption at 668 nm, chlorin e6 derivative 6 shows its Q_y absorption at 664 nm, for the opening of the isocyclic ring destroyed the coplanar effect of 13^1-keto group. Whereas PP-18 methyl ester 4, having a six-membered anhydride ring, shows its Q_y absorption at 698 nm due to the decrease of steric hindrance effect from five-memebered to sex-membered ring and another electron withdrawing group (C=O) situated at 15^1-position. The red shift of Q_y absorption from PP-18 methyl ester 4 (699 nm) to PPI derivative 15A (708 nm) can be explained by the difference of electron withdrawing effect between imide (15A) and anhydride (4) groups.

Gold nanoparticles (GNPs) delivery

For selective targeting in PDT, NPs have been attracted much

attention due to their unique optical properties derived from localized surface plasmon resonances.[83] NPs can increase hydrophilic affinity and have easy surface modification for enhancing chemical or biochemical properties, and finally, preferentially accumulated in tumor sites through the so-called "enhanced permeability and retention" effect.[84] Among NPs, GNPs have many advantages for promising delivery as well as for selective localized photothermal heating of cancer cells, called photothermal therapy (PTT).[85] Cheng et al.[86] have used GNPs conjugates with silicon Pc 4 as PS carriers for *in vivo* delivery of the PS resulting in surprisingly efficient release and penetration of the PS into the tumor .

Ionic liquids (ILs) have attracted the attention in various application areas, such as catalysis, synthesis, gas absorption, and analysis, based on attractive properties.[87] Generally ILs are defined as salts composed of discrete cations and anions with melting points below 100°C, and most of them have liquid form at room temperature.[88] For the synthesis of metal NPs, ILs are efficient capping agents as well as solvents to stabilize the formation of NPs.[89,90]

Most of PSs are hydrophobic which can lead aggregation that reduces solubility in aqueous system; however, highly water soluble (hydrophilic) PSs may have limit to penetrate through the tissue and cell membranes, resulting in poor cellular uptake.[91,92] Therefore, a combination synthesis (PS-GNPs conjugates) of IL type PS and GNPs could be a solution to allow high cellular uptake of PSs in tumor site.[93]

Chlorin- and porphyrin-based PS-GNPs conjugates have been prepared by us[94-96] and another group,[97] respectively. We developed straightforward synthetic method of PS-GNPs conjugate using IL type PS with *N*-methyl-*D*-glucamine (NMGA; Pu-18-NMGA) (Fig. 9).[95] In this synthesis, the hydroxyl groups of NMGA play important roles as a reducing agent as well as a stabilizer through the electrically charged functional groups (i.e., carboxylate and amine groups) in forming the PS-GNPs conjugate. Furthermore, we evaluated *in vitro* anticancer efficacy of the conjugate and its free PS against A549 lung cancer cell lines, which showed that the PS-GNPs conjugate has three times higher photodynamic efficacy relative to free IL type PS (Fig. 10).

It is noted that the size of the GNPs plays a big role in their uptake at the cellular level leading to different PDT activity. We have synthesized various sizes of PS-GNPs conjugates using a simple single-step synthesis from different molar ratios of $HAuCl_4$/PS without adding any particular reducing agents and surfactants, and showed size effect allowed different photodynamic activity results of the conjugates as an important factor for PDT.[96] We revealed that PDT *in vitro* activity of synthesized PS-GNPs conjugates was higher compared to free PS because of good transport of the PS into the cells by using size effect. Conjugate a based on molar ratio between $HAuCl_4$ and PS was 1:2 that exhibits best PDT efficiency than other conjugates having different molar ratios. This result could be useful for synthesis of new PS and PS-GNPs conjugates having different size as well as for developing good relationship between PDT activity and size effect of GNPs in aqueous media.

Combination therapy

PDT with anticancer agents

PDT *in vivo* reduces tumor cells through direct photo damage of cellular components, but it is often not achieved complete tumor eradication, predominantly due to nonhomogeneous distribution of the PS within the tumor and the limited availability of oxygen within the target tissue during irradiation.[2,20] Therefore, combination therapy combining PDT and other chemotherapeutic agents was used to achieve substantial gains in tumor destruction and long-term tumor control.[3]

One strategy in the context of combination therapy to develop new generation PSs is related to conjugates that combined PS and other chemotherapeutic agents together to increase the lethality of PDT treatment. It was found that the water soluble complexes are the most promising new porphyrin platinum conjugates.[98,99] The hypothesis for the use of such systems is based not only on the combined effect of PDT and cytostatic activities, but also on the porphyrin-mediated targeting of tumors.[100] Combination chemotherapy and PDT with free SOS and Mce6, their nontargeted and Fab'-targeted

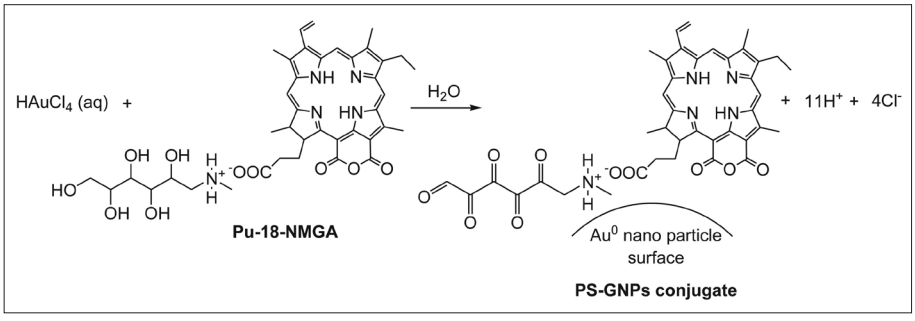

Fig. 9. Synthetic pathway of Pu-18-N-methyl-D-glucamine (NMGA) conjugated to gold nanoparticles (GNPs). PS, photosensitizer. Adapted from Lkhagvadulam et al. J Porphyr Phthalocyanines 2012;16:331-340, with permission from World Scientific Publishing Co.[95]

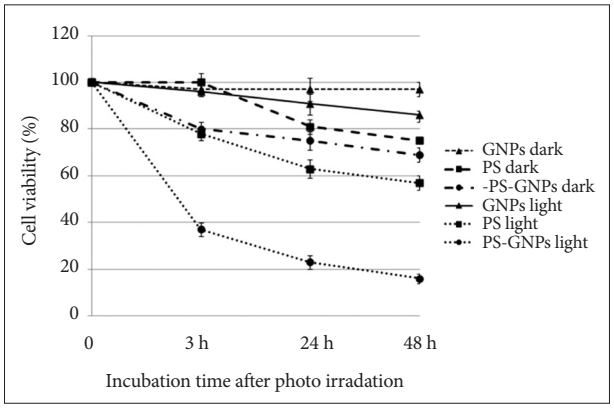

Fig. 10. Cell viability (%) of Pu-18-*N*-methyl-*D*-glucamine (photosensitizer, PS), PS-gold nanoparticles (GNPs) conjugate (PS-GNPs), and citrate-GNPs (GNPs) (5.5 μg/mL concentration of PS) treated A549 cells by exposure to an irradiation at 670 to 710 nm (2 J/cm^2) for 15 minutes. Error bars represent the standard deviation of three replicate experiments. Adapted from Lkhagvadulam et al. J Porphyr Phthalocyanines 2012;16:331-340, with permission from World Scientific Publishing Co.[95]

HPMA copolymer conjugates in human ovarian carcinoma OVCAR-3 cells was evaluated.[101] Sequential combinations of these therapeutics produced very strong synergy to near additivity in the treatment of OVCAR-3 cells.[101]

Another strategy is related to pro-oxidants. It is well known that antioxidants can prevent carcinomatous change via prevention of oxidative damage of DNA.[102] However, one of the most important biological effects in PDT process is the lethal oxidative stress induced by ROS. Interestingly, some studies have shown the combinational use of certain antioxidants can also enhance the activity of PDT, in which process antioxidants exhibit pro-oxidant activities, especially in the presence of catalytic metals.[103] Several research groups have reported results on the PDT enhancing activities of certain antioxidant molecules, such as ascorbate,[104] 3(2)-tetra-butyl-4-hydroxyanisole,[105] epigallocatechin-3-gallate,[106] α-tocopherol,[107] and trolox ([±]- 6-hydroxyl-2, 5, 7, 8-tetramethyl chromane-2-carboxylic acid, a water soluble vitamin E analogue).[108] Based on these intriguing results, some antioxidant carrier sensitizers (ACSs) which conjugated PSs and antioxidants together were designed and studied for their photodynamic anticancer[109] and antibacterial activities.[110] It was noted that the PDT effect of such ACSs is based on the so called type III (or MTO) mechanism which increases the singlet oxygen production via inhibition of the interaction between triplet excited PS and native free radicals.[109]

PDT and PTT

As a cancer therapy, hyperthermia relies on the localized heating of tumors at more than 43°C.[111] Near infrared (NIR) wavelengths (700 to 850 nm) absorption to the NPs has shown enhanced effect called as a PTT.[112] NIR irradiation has an optimal penetration into tumor tissues (a few centimeters) and strong absorption of NPs that allow low power need for enough therapeutic result with no significant heating of normal tissues.[113] Currently, there are two main groups of photothermal agents. Gold nanostructures (nanoshells, nanorods, and nanocages) can induce surface plasmon resonance and can afford enhanced optical and electronic properties, making it useful in biological and medical applications.[114] In addition, the GNPs have shown its excellent antiphotobleaching effect at strong illumination and are chemically inert under physiological conditions.[115] And carbon nanotubes are able to generate the photothermal ablation of cancer cells with NIR light with no damage of normal tissues based on the low scattering and low absorption in NIR region.[116]

Melancon et al.[117] have shown that hollow gold nanospheres activated by NIR (808 nm at 4 W/cm^2 for 3 minutes) increased temperature above 54°C *in vitro*. Ke et al.[118] have used gold nanoshelled microcapsules (GNS-MCs) for PTT and ultrasound contrast imaging, in which the temperature was more than 42°C with 0.3 to 0.5 mg/mL GNS-MCs (808 nm at 2 to 8 W/cm^2 for 10 minutes by continuous wave (CW) fiber-coupled diode laser) for sufficient cell killing. Yang et al.[119] reported NIR photothermal ablation of cancer cells using polyaniline NPs that NIR irradiation allowed higher temperature rise (54.8°C at 808 nm and 2.45 W/cm^2 for 5 minutes) compared to pure water (6.6°C).

Previously, we developed GNPs consisted of IL type PSs for increasing affinity in aqueous media, in which as appropriate PS delivery carrier the GNPs have shown better photodynamic effect than free PSs.[95,96] In addition, the GNPs showed long wavelength absorptions more than 750 nm,[94-96] so evaluation of photothermal effect using the GNPs is currently under way in our laboratory.

LIGHT DELIVERY SYSTEM

The clinical approach of PDT depends on the appropriate light delivery and sufficient PS concentration in the presence of oxygen to the target tumor tissue.[120,121] All the main factors for PDT light delivery have an important role to support successful treatments resulting in excellent therapeutic effect.[120-122] The development of light sources, generally lasers or light emitting diodes (LEDs), and appropriate delivery devices with the dosimetric parameters are key components of the clinical practice of PDT. Accurate delivery of the light to the exact tumor tissue could be accomplished by a technical combination of suitable light sources and optimal fiberoptic delivery devices consist of quartz fibers with cylindrical diffusing tips of various lengths and flexibility or fiberoptics with a lens. The light delivery devices should be clinically oriented to give en-

ough dosimetry with standardization showing maximum efficiency with minimum normal tissue injury.[122] For widespread use of PDT, the major barriers is the cost, complexity and the availability of the laser and light delivery systems. Among them, the lack of advanced light delivery technology is significantly important.[123]

Laser systems for PDT

Mang have reported development of light delivery systems for advanced PDT technology as follows.[123]

Argon/dye lasers

Argon/dye laser is the standard and widely used source for clinical PDT. It is capable of delivering 1 to 7 W of CW 630 nm light depending on the model and make of the system. High power systems have large frame units made by manufacturers such as Spectra Physics (Mountain View, CA, USA) and Coherent (Santa Clara, CA, USA). Typical powers of the argon laser are 15 to 20 W range, which could convert enough energy via the dye laser to generate more than 7 W. Coherent designed a clinical argon/dye laser system for PDT using 630 nm for the activation of Photofrin (2 W usable power).

Metal vapor lasers

These lasers are portable and do not require specialized electrical supply or water cooling. Also, they do not need coupling to a dye laser to generate suitable output power. The gold vapor laser could generate a 628 nm wavelength with sufficient power for clinical or experimental PDT studies with a pulsed output at 5 to 15 kHz frequency.[124] However, this laser is expensive due to the need for regular charges of gold to maintain the output power. Otherwise, a copper vapor laser costs less to maintain, however, this laser needs a dye laser module in the package. A major disadvantage of these metal vapor lasers is the need for long warm-up and cool down periods, which makes it impractical for clinical use.

KTP:YAG/dye lasers

The Laserscope 800 series (Laserscope, San Jose, CA, USA) operates at 1,064 nm and at the frequency-doubled phase allowing a quasi-CW (25 kHz) laser beam at 532 nm. The wavelength is delivered through fiberoptic connections to a dye laser, generating a beam at 630 nm. This system produces pulsed light and has several advantages, such as low cost, portability, durability and easy use.

Diode lasers

Diomed Inc. (Andover, MA, USA) obtained FDA approval of 630 nm diode laser for use of Photofrin in esophageal and lung malignancies in 2000. Diode lasers are semiconductor light sources without the optical configurations of the standard laser systems used in PDT. This system has advantages, such as easy use in utilizing 120 V power and an air-cooling system, lightweight (portable), simple software, less expensiveness, and stable output power for long period. Biolitec (East Longmeadow, MA, USA) made a 652 nm diode laser and received approval in Europe, Ireland, and Norway for use of Foscan. The output power at the fiber optic tips is 2 to 2.5 W.

Nonlaser light sources

LED light is produced by a solid-state process (electroluminescence). An LED is a directional light source with the maximum emitted power in the direction perpendicular to the emitting surface. LED is compact, lightweight, and requires low energy to make the desired wavelengths of light.[125] Quantum Devices (Barnweld, WI, USA) and EXFO (Missassauga, ON, Canada) companies are main manufacturers of this system with output powers of up to 150 mW/cm^2 at various wavelengths (630, 670, and 690 nm).

Fiber optic delivery devices

Main purpose of a combination between the light source and delivery devices in PDT is to generate enough light illumination (optical power, W) at the appropriate wavelength for activation of PS and optimum penetration into the target tissue and the corresponding spatial light distribution in the tumor volume (various size and shape).[126] The light delivery lasers have advantages, such as easy coupling with fiber optics following direct delivery of homogeneous and ample amount of light to the target site. The design and development of fiberoptic delivery devices should be made with a few considerations, such as sufficient power delivery, compatibility with clinical instrumentation (i.e., endoscopes), and proper type of the fiberoptic delivery tip to correspond to tumor shape, volume size or cavitary area.

Cylindrical fibers

The most widely used fiberoptic light delivery device in PDT is cylindrical diffusing fiber tip which was manufactured by a few companies. The diffusers are available in lengths of 1 to 9 cm range depending on the specific application. For the use of the standard cylindrical diffusing fiber, two light delivery methods have been developed: intraluminal irradiation techniques used for the lung and esophagus, and interstitial illumination methods to deliver adequate light doses to the target tumor volume.

Balloon catheters and Lens fiberoptics

For intraluminal dosimetry within the esophagus, the cylindrical light diffuser is introduced into the balloon catheter

which is inflated to about 25 mm diameter using a pressure of about 20 mm Hg. For uniform surface illumination, a micro or macro lens could be attached at the end of the fiber.

Light dose and wave type

Grossweiner has developed four PDT light dosimetry models for the necrosis depth calculation: front surface–a uniform irradiance incident beam delivered by an external source; point surface–an isotropic source centered in a spherical cavity; cylindrical surface–a line source centered in a cylindrical lumen; and cylindrical insertion–a line source embedded in the tumor tissue.[127]

In order to establish increased PDT efficiency, many groups investigated important effects of light dose and fluence rate.[121,128-130] Consequently, high light dose with medium fluence rate is an excellent combination for a solid tumor treatment.[121,129]

A new incoherent, high intensity pulsed light delivery system was tested *in vivo* (female BALB/c mice) using argon ion laser at total dose of 90 to 240 J/cm^2 and 600 to 800 nm wavelength range.[131] The tumor growth inhibition and the amount of edema (side effect) were directly dependent on the light dose used.

Tudge et al.[128] have reported that haematoporphyrin derivative (HpD, 0 to 20 mg/kg) with 630 nm irradiation by laser light (total energy dose 0 to 1,200 J/cm^2, fluence rate 625, 3,125, or 9,375 mW/cm^2) was used against brain tumor. In normal brain tissue, failure of drug light dose reciprocity indicated that photobleaching was occurred. Selective tumor kill was obtained at 1.0 mg/kg HpD and 800 J/cm^2 light dose corresponding to 2.2 mm depth of tumor necrosis. And the slower light delivery increased tumor kill based on allowing greater production of free oxygen radicals.

Lapchak group has investigated both continuous and pulse frequency light delivery modes in rabbits, resulting in statistically significant clinical improvement by using pulse therapies.[132] They used power density of 7.5 mW/cm^2 and 2 minutes treatment for both continuous and pulse waves, and calculated the effective stroke dose for clot weight (mg) which produces neurological deficits in 50% of rabbits (P_{50} values).

For clinical application, Bowen disease on both right and left cheeks was treated by PDT using two light deliveries, 378 J/cm^2 at 90 mW/cm^2 for 7 minutes and 13.8 J/cm^2 at 11 mW/cm^2 for 20 minutes exposure.[120] 5-Aminolevulinic acid (ALA) was delivered by nanossomic vehicle and a second PDT was treated two weeks after the first PDT. The neoplastic area healed in 15 days and histologic cure was achieved three months after the treatment, and no recurrence has occurred after a 6 months follow-up period.

Light applicator (diffuser)

In order to solve a problem of inadequate light delivery in brain tissue, indwelling balloon applicator having great flexibility for long-term implantation was developed by Madsen et al.[129] In brain tissue, the light penetration is limited and, as a result, long treatment time was required for sufficient light doses to depths of 1 to 2 cm in the resection cavity. They used human glioma spheroid and 5-ALA, 100 or 1,000 μg/mL as a PS. The spheroid survival was monitored as a function of light fluence rate (5 to 200 mW/cm^2, 635 nm irradiation using argon ion-pumped dye laser). Higher fluence (50 J/cm^2) and lower fluence rates (10 mW/cm^2, longer treatment times) afforded more efficient results in many cases. In addition, the repeated PDT treatments were more effective than single (one time) procedure to suppress the regrowth (about 1 week after the last PDT) of surviving spheroids.

Lights can penetrate lung (cystic fibrosis) tissue only by a few millimeters due to the solid lung tumor blocking the light penetration effectively.[133-135] Cassidy et al.[134] conducted multiple lobe irradiation *in vivo* by inserting a fiber optic probe coupled with a helium-neon laser with a diffuser tip into the lobe of the pulmonary tissue, which resulted in up to 11% of the total light dose penetrating through pulmonary parenchymal tissue. Longer wavelength enabled increased light dose delivery through porcine pulmonary tissue (785 nm laser increased about 23% compared to 663 nm laser).

Light delivery throughout the entire organ using internal reflection to allow fiberoptic cables (light pipes) was studied by Friedberg et al.[135] They used *ex vivo* sheep tracheas and lungs were filled with various substances (air, water, and mineral oil) for varying refractive indices. Filling with mineral oil in the lung showed entire bright, dramatic, and near uniform illumination. This suggests that it is possible to deliver light around bends and through a branched network.

It is available to apply light delivery in geometrically complex sites, such as the nasopharynx and other nonuniform surfaces by using flexible light delivery system. Nyst et al.[130] developed a flexible silicone applicator (using bending of the cylindrical diffuser) incorporating light delivery and dosimetry fibers which can deliver the light fluence into the nasopharynx. They measured fluence rate variations at the applicator surface during PDT, which showed that the fluence rate distribution was homogeneous.

For the treatment of luminal lesions, a combination of stenting and PDT is realizable based on easy placement of the metal stents. Wang et al.[136] have shown that PDT is useful to control both tumor ingrowth and overgrowth through a stent using laser light delivery by a cylindrical diffuser and endoscope. They have compared light delivery effect (light transmittance) using various kinds of stents (biliary, esophageal,

and bronchial stents) with different size for pig biliary duct and esophageal wall tissues.

Kruijt et al.[121] showed a light applicator (diffuser) based on standard anoscopy equipment with all fiber optics, a light treatment fiber and fiber optic probes, to monitor blood saturation, blood volume, fluorescence and fluence rate for light delivery and monitoring of PDT of intra-anal intraepithelial neoplasia without changing the light treatment protocol. During illumination, the blood saturation was almost constant; otherwise, the blood volume showed slight wave behavior. Lower fluence rate (45 to 50 mW/cm^2) is more effective than higher fluence rate (100 to 245 mW/cm^2) since it prevents rapid oxygen depletion and low blood saturations during illumination.

Light delivery and oxygen supply in the target tissue

PDT process enables target tissue destruction by a combination of direct cell killing and vascular damage (i.e., blood coagulation and vascular closure).[137] For effective PDT, environment oxygen concentration of the target tissue is a significantly important issue. After PDT, vascular damage could allow tumor cell ablation by anoxia from obstruction of blood vessels. During PDT, however, vascular damage induced by PDT may allow tumor hypoxia from local oxygen consumption which could cause a neovascularization, and prevent efficient PDT treatment, leading to a tumor recurrence. It is necessary, therefore, to supply oxygen during PDT for maintenance of tumor oxygenation for improvement of tumor response based on increased ROS amount. Chen group introduced heparin to improve light delivery and oxygen supply in a solid tumor model, in which heparin administration before PDT delayed blood coagulation and vascular closure and thus improved the blood perfusion (inhibition of thrombosis formation) and light transmission.[137] For tumor oxygenation, hyperoxygenation and carbogen (a mixed gas of 30% CO_2 and 70% O_2) breathing are very useful techniques *in vivo* system.[138] In addition, increased oxygen concentration could allow enhanced penetration of red light because oxyhemoglobin has lower red light absorbance than that of deoxyhemoglobin.[138]

Computer-aided light delivery

To reduce normal tissue damage, light and the PS should be delivered to the target tissue or organ with high selectivity. In addition, more accurate light and drug delivery, and real-time dosimetry for monitoring changes in light fluence during PDT are need. Xiao et al.[139] developed a computer driven switch (pulse) system with intra-arterial administration of PS (BPD) for prostate cancer treatment of dogs. The light delivery was carried out using seven optic fibers with 1.5 cm cylindrical light diffusing tips, for which multiple fibers were used to cover the entire prostate treatment since prostate cancer is usually multifocal. The total delivered light dose to the prostate was 900 J at fluence rate 100 mW/cm (or less). The average prostate volume was successfully decreased (71% at 3 months and 56% after 6 months), which was confirmed by microscopic evaluation showing comprehensive destruction of the prostate (hemorrhagic and coagulative necrosis, glandular cell degeneration with sloughing, stromal edema and vascular stasis).

The prostate has irregular shape, which is why a multifocal treatment is useful. It is hard to accomplish a complete glandular ablation with PDT; therefore, transurethral light delivery (circular in distribution) is not suitable for prostate cancer treatment. Monte Carlo simulations are useful in tissue optical characterization and PDT modeling; however, this method is time-consuming and impractical for clinical application.[140] Jankun et al.[141] developed a computer-aided light delivery method that can calculate the volume of ablated tissue and predict the outcome on a three-dimensional virtual model of the prostate. They predicted the volume and geometry of photoinjury to the prostate during PDT, and compared with observed values of radii of prostate photo-ablation within ±2 mm differences between them. The shape and volume of phtotoablation of the prostate depends on the spatial distribution of the effective attenuation coefficient (μ_{eff}/cm) and the properties of the light diffusers (different among the various manufactures) (200 J/cm [200 mW/cm, 1,000 seconds]).

Light delivery and PTT

Pulsed PTT against pigmented B16 mice melanoma tumors was investigated using a Photodyne incoherent light delivery system.[142] After tumor heating at light doses (60 to 120 J/cm^2 with 0.6 J/cm^2 per pulse), average temperature reached 41°C to 44°C during photo irradiation (600 to 800 nm), and tumor volume [$V=\pi/6(D_1\times D_2\times D_3)$, where D_1, D_2 and D_3 are three orthogonal diameters] and the tumor growth inhibition ratio ($TGIR=[(k_c-k_t)/k_c]100\%$, where k_c and k_t are constants for control and treatment groups, respectively) were measured. The damage effects (edema and destruction of the basement membrane, mitochondrial damage and destruction of melanosomes, and no nuclear damage) and tumor necrosis depth were associated with the light dose used. The highest light dose (120 J/cm^2) induced hyperthermia showing an excellent results of irreversible damage and tumor regrowth inhibition.

CONCLUSIONS

PDT has obvious advantages over other conventional cancer treatments such as chemotherapy, surgery, and radioth-

erapy, in that it can achieve dual selectivity, which is based on the selective accumulation of the PS in the tumor or other diseased tissue and on the spatially confined and focused delivering of light into the target tissue. In order to overcome undesired side effects of PDT, a number of the second and third generation PSs have been developed, especially chlorophyll Chl derivatives for both economic and environmental advantages of such naturally occurring chlorins. The development of PSs is likely to focus on increasing therapeutic efficacy and selectivity (targeting) for malignant tissues. A combination therapy, such as PDT with anticancer agents or PDT with PTT, is useful in order to significantly reduce drug dose and prevent tumor recurrences for complete therapeutic effect. Advanced light delivery technology shows successful investigations *in vitro* and *in vivo* for further clinical applications in PDT.

Conflicts of Interest

The authors have no financial conflicts of interest.

Acknowledgments

This research was supported by the BK21 Project and the National Research Foundation (NRF) of Korea Grant funded by the Ministry of Education, Science and Technology (NRF-2011-0007082 and NRF-2009-353-C00055). Also this work was supported by the Inje Research and Scholarship Foundation in 2009.

REFERENCES

1. Szaciłowski K, Macyk W, Drzewiecka-Matuszek A, Brindell M, Stochel G. Bioinorganic photochemistry: frontiers and mechanisms. Chem Rev 2005;105:2647-2694.
2. Pandey RK, Zheng G. Porphyrins as photosensitizers in photodynamic therapy. In: Kadish KM, Smith KM, Guilard R, eds. The Porphyrin Handbook. Boston: Academic Press; 2000. p.157-230.
3. Zuluaga MF, Lange N. Combination of photodynamic therapy with anti-cancer agents. Curr Med Chem 2008;15:1655-1673.
4. Juarranz A, Jaén P, Sanz-Rodríguez F, Cuevas J, González S. Photodynamic therapy of cancer. Basic principles and applications. Clin Transl Oncol 2008;10:148-154.
5. Dougherty TJ, Henderson BW, Schwartz S, Winkelman JW, Lipson RL. Historical perspective. In: Henderson BW, Dougherty TJ, eds. Photodynamic Therapy: Basic Principles and Clinical Applications. New York: M. Dekker; 1992. p.1-15.
6. Dougherty TJ, Grindey GB, Fiel R, Weishaupt KR, Boyle DG. Photoradiation therapy. II. Cure of animal tumors with hematoporphyrin and light. J Natl Cancer Inst 1975;55:115-121.
7. Orenstein A, Kostenich G, Roitman L, et al. A comparative study of tissue distribution and photodynamic therapy selectivity of chlorin e6, photofrin II and ALA-induced protoporphyrin IX in a colon carcinoma model. Br J Cancer 1996;73:937-944.
8. Spikes JD. Chlorins as photosensitizers in biology and medicine. J Photochem Photobiol B 1990;6:259-274.
9. Baas P, van Mansom I, van Tinteren H, Stewart FA, van Zandwijk N. Effect of N-acetylcysteine on photofrin-induced skin photosensitivity in patients. Lasers Surg Med 1995;16:359-367.
10. Kessel D, Thompson P. Purification and analysis of hematoporphyrin and hematoporphyrin derivative by gel exclusion and reverse-phase chromatography. Photochem Photobiol 1987;46:1023-1025.
11. Castanoa AP, Demidova TN, Hamblin MR. Mechanisms in photodynamic therapy: part one: photosensitizers, photochemistry and cellular localization. Photodiagnosis Photodyn Ther 2004;1:279-293.
12. Sternberg ED, Dolphin D, Brückner C. Porphyrin-based photosensitizers for use in photodynamic therapy. Tetrahedron 1998;54:4151-4202.
13. Foote CS. Definition of type I and type II photosensitized oxidation. Photochem Photobiol 1991;54:659.
14. Gál D. Effect of photosensitizers in chemical and biological processes: the MTO mechanism in photodynamic therapy. Biochem Biophys Res Commun 1992;186:1032-1036.
15. Vidóczy T, Elzemzam S, Gál D. Physico-chemical modeling of the role of free radicals in photo-dynamic therapy. I. utilization of quantum yield data of singlet oxygen formation for the study of the interaction between excited photosensitizer and stable free radicals. Biochem Biophys Res Commun 1992;189:1548-1552.
16. Gál D, Kriska T, Maltseva E. In vivo experimental studies on the role of free radicals in photodynamic therapy. III. photodynamic effect on free radicals generated in cell cultures. Biochem Biophys Res Commun 1997;233:173-176.
17. Figge FH, Weiland GS, Manganiello LO. Cancer detection and therapy: affinity of neoplastic, embryonic, and traumatized tissues for porphyrins and metalloporphyrins. Proc Soc Exp Biol Med 1948;68:640.
18. Hamblin MR, Newman EL. On the mechanism of the tumour-localising effect in photodynamic therapy. J Photochem Photobiol B 1994; 23:3-8.
19. Boyle RW, Dolphin D. Structure and biodistribution relationships of photodynamic sensitizers. Photochem Photobiol 1996;64:469-485.
20. Castano AP, Demidova TN, Hamblin MR. Mechanisms in photodynamic therapy: part three: photosensitizer pharmacokinetics, biodistribution, tumor localization and modes of tumor destruction. Photodiagnosis Photodyn Ther 2005;2:91-106.
21. Yuan F, Leunig M, Berk DA, Jain RK. Microvascular permeability of albumin, vascular surface area, and vascular volume measured in human adenocarcinoma LS174T using dorsal chamber in SCID mice. Microvasc Res 1993;45:269-289.
22. Pottier R, Kennedy JC. The possible role of ionic species in selective biodistribution of photochemotherapeutic agents toward neoplastic tissue. J Photochem Photobiol B 1990;8:1-16.
23. Allison BA, Pritchard PH, Levy JG. Evidence for low-density lipoprotein receptor-mediated uptake of benzoporphyrin derivative. Br J Cancer 1994;69:833-839.
24. Roberts WG, Hasan T. Role of neovasculature and vascular permeability on the tumor retention of photodynamic agents. Cancer Res 1992; 52:924-930.
25. Korbelik M, Krosl G. Photofrin accumulation in malignant and host cell populations of a murine fibrosarcoma. Photochem Photobiol 1995; 62:162-168.
26. Wendler G, Lindemann P, Lacapère JJ, Papadopoulos V. Protoporphyrin IX binding and transport by recombinant mouse PBR. Biochem Biophys Res Commun 2003;311:847-852.
27. Wilson BC, Jeeves WP, Lowe DM. In vivo and post mortem measurements of the attenuation spectra of light in mammalian tissues. Photochem Photobiol 1985;42:153-162.
28. Szacilowski K, Macyk W, Drzewiecka-Matuszek A, Brindell M, Stochel G. Bioinorganic photochemistry: frontiers and mechanisms. Chem Rev 2005;105:2647-2694.
29. O'Connor AE, Gallagher WM, Byrne AT. Porphyrin and nonporphyrin photosensitizers in oncology: preclinical and clinical advances in photodynamic therapy. Photochem Photobiol 2009;85:1053-1074.
30. Allison RR, Sibata CH. Oncologic photodynamic therapy photosensitizers: a clinical review. Photodiagnosis Photodyn Ther 2010;7:61-75.
31. Brandis AS, Salomon Y, Scherz A. Chlorophyll sensitizers in photodynamic therapy. In: Grimm B, Porra RJ, Rüdiger W, Scheer H, eds. Chlorophylls and Bacteriochlorophylls: Biochemistry, Biophysics, Functions and Applications. Dordrecht: Springer; 2006. p.461-483.
32. Pandey RK, Shiau FY, Sumlin AB, Dougherty TJ, Smith KM. Structure/activity relationships among photosensitizers related to pheophorbides

and bacteriopheophorbides. Bioorg Med Chem Lett 1992;2:491-496.
33. Bellnier DA, Henderson BW, Pandey RK, Potter WR, Dougherty TJ. Murine pharmacokinetics and antitumor efficacy of the photodynamic sensitizer 2-[1-hexyloxyethyl]-2-devinyl pyropheophorbide-a. J Photochem Photobiol B 1993;20:55-61.
34. Pandey RK, Sumlin AB, Constantine S, et al. Alkyl ether analogs of chlorophyll-a derivatives: part 1. synthesis, photophysical properties and photodynamic efficacy. Photochem Photobiol 1996;64:194-204.
35. Lobel J, MacDonald IJ, Ciesielski MJ, et al. 2-[1-hexyloxyethyl]-2-devinyl pyropheophorbide-a (HPPH) in a nude rat glioma model: implications for photodynamic therapy. Lasers Surg Med 2001;29:397-405.
36. Pandey RK, Herman CK. Shedding some light on tumours. Chem Ind 1998;18:739-743.
37. Clinicaltrials.gov. Photodynamic Therapy Using HPPH in Treating Patients With Advanced Non-Small Cell Lung Cancer That Blocks the Air Passages [Internet]. Bethesda: The U.S. National Institutes of Health; 2013 [updated 2013 Jan 10; cited 2013 Jan 21]. Available from: http://clinicaltrials.gov/ct2/show/NCT00528775.
38. Matsumura H, Akimoto J, Haraoka J, Aizawa K. Uptake and retention of the photosensitizer mono-L-asparthyl chlorine e6 in experimental malignant glioma. Lasers Med Sci 2008;23:237-245.
39. Kennedy JC, Nadeau P, Petryka ZJ, Pottier RH, Weagle G. Clearance times of porphyrin derivatives from mice as measured by in vivo fluorescence spectroscopy. Photochem Photobiol 1992;55:729-734.
40. Ando T, Irie K, Koshimizu K, et al. Synthesis, physicochemical properties and photocytotoxicity of five new δ-substituted chlorin e6 derivatives. Tetrahedron 1990;46:5921-5930.
41. Kato H, Furukawa K, Sato M, et al. Phase II clinical study of photodynamic therapy using mono-L-aspartyl chlorin e6 and diode laser for early superficial squamous cell carcinoma of the lung. Lung Cancer 2003;42:103-111.
42. Kujundzić M, Vogl TJ, Stimac D, et al. A Phase II safety and effect on time to tumor progression study of intratumoral light infusion technology using talaporfin sodium in patients with metastatic colorectal cancer. J Surg Oncol 2007;96:518-524.
43. Hoober JK, Sery TW, Yamamoto N. Photodynamic sensitizers from chlorophyll: purpurin-18 and chlorin p6. Photochem Photobiol 1988; 48:579-582.
44. Zenkevich E, Sagun E, Knyukshto V, et al. Photophysical and photochemical properties of potential porphyrin and chlorin photosensitizers for PDT. J Photochem Photobiol B 1996;33:171-180.
45. Zheng G, Aoudia M, Lee D, et al. Chlorin-based symmetrical and unsymmetrical dimers with amide linkages: effect of the substituents on photodynamic and photophysical properties. J Chem Soc Perkin Trans 1 2000;(24):3113-3121.
46. Smith KM, Lee SJ, Shiau FY, Pandey RK, Jagerovic N. Syntheses of chlorin and bacteriochlorin-type photosensitizers for photodynamic therapy. In: Spinelli P, Dal Fante M, Marchesini R, eds. Photodynamic Therapy and Biomedical Lasers. Amsterdam: Elsevier Science Publishers B.V.; 1992. p.769-773.
47. Pandey RK, Goswami LN, Chen Y, et al. Nature: a rich source for developing multifunctional agents. Tumor-imaging and photodynamic therapy. Lasers Surg Med 2006;38:445-467.
48. Zheng G, Potter WR, Sumlin A, Dougherty TJ, Pandey RK. Photosensitizers related to purpurin-18-N-alkylimides: a comparative in vivo tumoricidal ability of ester versus amide functionalities. Bioorg Med Chem Lett 2000;10:123-127.
49. Pandey RK, James NS, Chen Y, Missert J, Sajjad M. Bifunctional agents for imaging and therapy. Methods Mol Biol 2010;635:223-259.
50. Pandey RK, Constantine S, Tsuchida T, et al. Synthesis, photophysical properties, in vivo photosensitizing efficacy, and human serum albumin binding properties of some novel bacteriochlorins. J Med Chem 1997; 40:2770-2779.
51. Mettath S, Shibata M, Alderfer JL, et al. Synthesis and spectroscopic properties of novel benzochlorins derived from chlorophyll a. J Org Chem 1998;63:1646-1656.
52. Li G, Graham A, Chen Y, et al. Synthesis, comparative photosensitizing efficacy, human serum albumin (site II) binding ability, and intracellular localization characteristics of novel benzobacteriochlorins derived from vic-dihydroxybacteriochlorins. J Med Chem 2003;46:5349-5359.
53. Zheng X, Pandey RK. Porphyrin-carbohydrate conjugates: impact of carbohydrate moieties in photodynamic therapy (PDT). Anticancer Agents Med Chem 2008;8:241-268.
54. Shadidi M, Sioud M. Selective targeting of cancer cells using synthetic peptides. Drug Resist Updat 2003;6:363-371.
55. Polo L, Valduga G, Jori G, Reddi E. Low-density lipoprotein receptors in the uptake of tumour photosensitizers by human and rat transformed fibroblasts. Int J Biochem Cell Biol 2002;34:10-23.
56. Vrouenraets MB, Visser GW, Loup C, et al. Targeting of a hydrophilic photosensitizer by use of internalizing monoclonal antibodies: a new possibility for use in photodynamic therapy. Int J Cancer 2000;88:108-114.
57. Chatterjee DK, Fong LS, Zhang Y. Nanoparticles in photodynamic therapy: an emerging paradigm. Adv Drug Deliv Rev 2008;60:1627-1637.
58. Greco F, Vicent MJ. Polymer-drug conjugates: current status and future trends. Front Biosci 2008;13:2744-2756.
59. Zhang M, Zhang Z, Blessington D, et al. Pyropheophorbide 2-deoxyglucosamide: a new photosensitizer targeting glucose transporters. Bioconjug Chem 2003;14:709-714.
60. Pandey SK, Zheng X, Morgan J, et al. Purpurinimide carbohydrate conjugates: effect of the position of the carbohydrate moiety in photosensitizing efficacy. Mol Pharm 2007;4:448-464.
61. Zheng X, Morgan J, Pandey SK, et al. Conjugation of 2-(1'-hexyloxyethyl)-2-devinylpyropheophorbide-a (HPPH) to carbohydrates changes its subcellular distribution and enhances photodynamic activity in vivo. J Med Chem 2009;52:4306-4318.
62. Liu FT, Rabinovich GA. Galectins as modulators of tumour progression. Nat Rev Cancer 2005;5:29-41.
63. Stefflova K, Li H, Chen J, Zheng G. Peptide-based pharmacomodulation of a cancer-targeted optical imaging and photodynamic therapy agent. Bioconjug Chem 2007;18:379-388.
64. Chen J, Jarvi M, Lo PC, Stefflova K, Wilson BC, Zheng G. Using the singlet oxygen scavenging property of carotenoid in photodynamic molecular beacons to minimize photodamage to non-targeted cells. Photochem Photobiol Sci 2007;6:1311-1317.
65. Ogura S, Yazaki K, Yamaguchi K, Kamachi T, Okura I. Localization of poly-L-lysine-photosensitizer conjugate in nucleus. J Control Release 2005;103:1-6.
66. Tijerina M, Kopecková P, Kopecek J. Correlation of subcellular compartmentalization of HPMA copolymer-Mce6 conjugates with chemotherapeutic activity in human ovarian carcinoma cells. Pharm Res 2003; 20:728-737.
67. Gariépy J. The use of Shiga-like toxin 1 in cancer therapy. Crit Rev Oncol Hematol 2001;39:99-106.
68. Tarragó-Trani MT, Jiang S, Harich KC, Storrie B. Shiga-like toxin subunit B (SLTB)-enhanced delivery of chlorin e6 (Ce6) improves cell killing. Photochem Photobiol 2006;82:527-537.
69. Zheng G, Li H, Zhang M, Lund-Katz S, Chance B, Glickson JD. Low-density lipoprotein reconstituted by pyropheophorbide cholesteryl oleate as target-specific photosensitizer. Bioconjug Chem 2002;13:392-396.
70. Nikolaeva IA, Misharin AY, Ponomarev GV, Timofeev VP, Tkachev YV. Chlorin e6-cholesterol conjugate and its copper complex. Simple synthesis and entrapping in phospholipid vesicles. Bioorg Med Chem Lett 2010;20:2872-2875.
71. Roy I, Ohulchanskyy TY, Pudavar HE, et al. Ceramic-based nanoparticles entrapping water-insoluble photosensitizing anticancer drugs: a novel drug-carrier system for photodynamic therapy. J Am Chem Soc 2003;125:7860-7865.
72. Ohulchanskyy TY, Roy I, Goswami LN, et al. Organically modified silica

nanoparticles with covalently incorporated photosensitizer for photodynamic therapy of cancer. Nano Lett 2007;7:2835-2842.
73. Cinteza LO, Ohulchanskyy TY, Sahoo Y, Bergey EJ, Pandey RK, Prasad PN. Diacyllipid micelle-based nanocarrier for magnetically guided delivery of drugs in photodynamic therapy. Mol Pharm 2006;3:415-423.
74. Hynninen PH. Chemistry of chlorophylls: Modifications. In: Scheer H, ed. Chlorophylls. Boca Raton: CRC Press; 1991. p.145-209.
75. Smith KM, Goff DA, Simpson DJ. The meso substitution of chlorophyll derivatives: direct route for transformation of bacteriopheophorbides d into bacteriopheophorbides c. J Am Chem Soc 1985;107:4946-4954.
76. Falk JE, Smith KM. Porphyrins and Metalloporphyrins. Amsterdam: Elsevier; 1975.
77. Tamiaki H, Amakawa M, Shimono Y, Tanikaga R, Holzwarth AR, Schaffner K. Synthetic zinc and magnesium chlorin aggregates as models for supramolecular antenna complexes in chlorosomes of green photosynthetic bacteria. Photochem Photobiol 1996;63:92-99.
78. Kozyrev AN, Zheng G, Lazarou E, Dougherty TJ, Smith KM, Pandey RK. Syntheses of emeraldin and purpurin-18 analogs as target-specific photosensitizers for photodynamic therapy. Tetrahedron Lett 1997;38: 3335-3338.
79. Rungta A, Zheng G, Missert JR, Potter WR, Dougherty TJ, Pandey RK. Purpurinimides as photosensitizers: effect of the presence and position of the substituents in the in vivo photodynamic efficacy. Bioorg Med Chem Lett 2000;10:1463-1466.
80. Spikes JD, Bommer JC. Photobleaching of mono-L-aspartyl chlorin e6 (NPe6): a candidate sensitizer for the photodynamic therapy of tumors. Photochem Photobiol 1993;58:346-350.
81. Li G, Slansky A, Dobhal MP, et al. Chlorophyll-a analogues conjugated with aminobenzyl-DTPA as potential bifunctional agents for magnetic resonance imaging and photodynamic therapy. Bioconjug Chem 2005; 16:32-42.
82. Weiss C. Electronic absorption spectra of chlorophylls. In: Dolphin D, ed. The Porphyrins. New York: Academic Press; 1978. p.211-223.
83. Hutter E, Fendler JH. Exploitation of localized surface plasmon resonance. Adv Mater 2004;16:1685-1706.
84. Torchilin VP. Multifunctional nanocarriers. Adv Drug Deliv Rev 2006; 58:1532-1555.
85. Jain PK, Huang X, El-Sayed IH, El-Sayed MA. Noble metals on the nanoscale: optical and photothermal properties and some applications in imaging, sensing, biology, and medicine. Acc Chem Res 2008;41: 1578-1586.
86. Cheng Y, Meyers JD, Broome AM, Kenney ME, Basilion JP, Burda C. Deep penetration of a PDT drug into tumors by noncovalent drug-gold nanoparticle conjugates. J Am Chem Soc 2011;133:2583-2591.
87. Giernoth R. Task-specific ionic liquids. Angew Chem Int Ed Engl 2010; 49:2834-2839.
88. Wasserscheid P, Welton T. Ionic Liquids in Synthesis. Weinheim: Wiley-VCH; 2003.
89. Itoh H, Naka K, Chujo Y. Synthesis of gold nanoparticles modified with ionic liquid based on the imidazolium cation. J Am Chem Soc 2004; 126:3026-3027.
90. Kim KS, Choi S, Cha JH, Yeon SH, Lee H. Facile one-pot synthesis of gold nanoparticles using alcohol ionic liquids. J Mater Chem 2006; 16:1315-1317.
91. Pegaz B, Debefve E, Borle F, et al. Preclinical evaluation of a novel water-soluble chlorin E6 derivative (BLC 1010) as photosensitizer for the closure of the neovessels. Photochem Photobiol 2005;81:1505-1510.
92. Sengee GI, Badraa N, Shim YK. Synthesis and biological evaluation of new imidazolium and piperazinium salts of pyropheophorbide-a for photodynamic cancer therapy. Int J Mol Sci 2008;9:1407-1415.
93. Pissuwan D, Niidome T, Cortie MB. The forthcoming applications of gold nanoparticles in drug and gene delivery systems. J Control Release 2011;149:65-71.
94. Demberelnyamba D, Ariunaa M, Shim YK. Newly synthesized water soluble cholinium-purpurin photosensitizers and their stabilized gold nanoparticles as promising anticancer agents. Int J Mol Sci 2008;9: 864-871.
95. Lkhagvadulam B, Kim JH, Yoon I, Shim YK. Synthesis and photodynamic activities of novel water soluble purpurin-18-N-methyl-D-glucamine photosensitizer and its gold nanoparticles conjugate. J Porphyr Phthalocyanines 2012;16:331-340.
96. Lkhagvadulam B, Kim JH, Yoon I, Shim YK. Size-dependent photodynamic activity of gold nanoparticles conjugate of water soluble purpurin-18-N-methyl-D-glucamine. BioMed Res Int 2013;2013:720579.
97. Gamaleia NF, Shishko ED, Dolinsky GA, Shcherbakov AB, Usatenko AV, Kholin VV. Photodynamic activity of hematoporphyrin conjugates with gold nanoparticles: experiments in vitro. Exp Oncol 2010;32:44-47.
98. Lottner C, Bart KC, Bernhardt G, Brunner H. Soluble tetraarylporphyrin-platinum conjugates as cytotoxic and phototoxic antitumor agents. J Med Chem 2002;45:2079-2089.
99. Lottner C, Bart KC, Bernhardt G, Brunner H. Hematoporphyrin-derived soluble porphyrin-platinum conjugates with combined cytotoxic and phototoxic antitumor activity. J Med Chem 2002;45:2064-2078.
100. Lottner C, Knuechel R, Bernhardt G, Brunner H. Combined chemotherapeutic and photodynamic treatment on human bladder cells by hematoporphyrin-platinum(II) conjugates. Cancer Lett 2004;203:171-180.
101. Hongrapipat J, Kopecková P, Liu J, Prakongpan S, Kopecek J. Combination chemotherapy and photodynamic therapy with fab' fragment targeted HPMA copolymer conjugates in human ovarian carcinoma cells. Mol Pharm 2008;5:696-709.
102. Frank J, Flaccus A, Schwarz C, Lambert C, Biesalski HK. Ascorbic acid suppresses cell death in rat DS-sarcoma cancer cells induced by 5-aminolevulinic acid-based photodynamic therapy. Free Radic Biol Med 2006;40:827-836.
103. Jakus J, Farkas O. Photosensitizers and antioxidants: a way to new drugs? Photochem Photobiol Sci 2005;4:694-698.
104. Kaliya OL, Lukyanets EA, Vorozhtsov GN. Catalysis and photocatalysis by phthalocyanines for technology, ecology and medicine. J Porphyr Phthalocyanines 1999;3:592-610.
105. Shevchuk I, Chekulayev V, Chekulayeva L. Enhancement of the efficiency of photodynamic therapy of tumours by t-butyl-4-hydroxyanisole. J Photochem Photobiol B 1998;45:136-143.
106. Raish M, Husain SZ, Bae SM, et al. Photodynamic therapy in combination with green tea polyphenol EGCG enhances antitumor efficacy in human papillomavirus 16 (E6/E7) immortalized tumor cells. J Appl Res 2010;10:58-67.
107. Melnikova V, Bezdetnaya L, Belitchenko I, Potapenko A, Merlin JL, Guillemin F. Meta-tetra(hydroxyphenyl)chlorin-sensitized photodynamic damage of cultured tumor and normal cells in the presence of high concentrations of alpha-tocopherol. Cancer Lett 1999;139:89-95.
108. Melnikova VO, Bezdetnaya LN, Brault D, Potapenko AY, Guillemin F. Enhancement of meta-tetrahydroxyphenylchlorin-sensitized photodynamic treatment on human tumor xenografts using a water-soluble vitamin E analogue, Trolox. Int J Cancer 2000;88:798-803.
109. Kriska T, Jakus J, Keszler A, Vanyur R, Nemeth A, Gal D. Type III photosensitization: attempt for quantification and a way toward new sensitizers. In: Ehrenberg B, Berg K, eds. Photochemotherapy of Cancer and Other Diseases. [place unknown]: SPIE Proceedings Vol. 3563; 1999. p.11-17.
110. Ashkenazi H, Nitzan Y, Gál D. Photodynamic effects of antioxidant substituted porphyrin photosensitizers on gram-positive and -negative bacterial. Photochem Photobiol 2003;77:186-191.
111. Pankhurst QA, Connolly J, Jones SK, Dobson J. Applications of magnetic nanoparticles in biomedicine. J Phys D Appl Phys 2003;36:R167-R181.
112. Park JH, von Maltzahn G, Ong LL, et al. Cooperative nanoparticles for tumor detection and photothermally triggered drug delivery. Adv Mater 2010;22:880-885.
113. Weissleder R. A clearer vision for in vivo imaging. Nat Biotechnol 2001;

19:316-317.
114. Lee J, Yang J, Ko H, et al. Multifunctional magnetic gold nanocomposites: human epithelial cancer detection via magnetic resonance imaging and localized synchronous therapy. Adv Funct Mater 2008;18:258-264.
115. Durr NJ, Larson T, Smith DK, Korgel BA, Sokolov K, Ben-Yakar A. Two-photon luminescence imaging of cancer cells using molecularly targeted gold nanorods. Nano Lett 2007;7:941-945.
116. Moon HK, Lee SH, Choi HC. In vivo near-infrared mediated tumor destruction by photothermal effect of carbon nanotubes. ACS Nano 2009; 3:3707-3713.
117. Melancon MP, Elliott AM, Shetty A, Huang Q, Stafford RJ, Li C. Near-infrared light modulated photothermal effect increases vascular perfusion and enhances polymeric drug delivery. J Control Release 2011;156: 265-272.
118. Ke H, Wang J, Dai Z, et al. Gold-nanoshelled microcapsules: a theranostic agent for ultrasound contrast imaging and photothermal therapy. Angew Chem Int Ed Engl 2011;50:3017-3021.
119. Yang J, Choi J, Bang D, et al. Convertible organic nanoparticles for near-infrared photothermal ablation of cancer cells. Angew Chem Int Ed Engl 2011;50:441-444.
120. Passos SK, Tedesco AC, Eid DR, Lacava ZG. Bowen disease treated with PDT using ALA in nanostructured vehicle and two light deliveries: a case report. J Am Acad Dermatol 2011;64(2 Suppl 1):AB141.
121. Kruijt B, van der Snoek EM, Sterenborg HJ, Amelink A, Robinson DJ. A dedicated applicator for light delivery and monitoring of PDT of intra-anal intraepithelial neoplasia. Photodiagnosis Photodyn Ther 2010; 7:3-9.
122. Mang TS. Light sources and delivery devices for photodynamic therapy. Photodiagnosis Photodyn Ther 2009;6:147.
123. Mang TS. Lasers and light sources for PDT: past, present and future. Photodiagnosis Photodyn Ther 2004;1:43-48.
124. Panjehpour M, Overholt BF, Haydek JM. Light sources and delivery devices for photodynamic therapy in the gastrointestinal tract. Gastrointest Endosc Clin N Am 2000;10:513-532.
125. Floyd TL. Electric Circuit Fundamentals. 2nd ed. New York: Merrill; 1991.
126. Star WM, Wilson BC, Patterson MS. Light delivery and optical dosimetry in photodynamic therapy of solid tumors. In: Henderson BW, Dougherty TJ, eds. Photodynamic Therapy: Basic Principles and Clinical Applications. New York: M. Dekker; 1992. p.335-368.
127. Grossweiner LI. PDT light dosimetry revisited. J Photochem Photobiol B 1997;38:258-268.
128. Tudge SH, Kaye AH, Hill JS. Modulation of light delivery in photodynamic therapy of brain tumours. J Clin Neurosci 1999;6:227-232.
129. Madsen SJ, Sun CH, Tromberg BJ, Hirschberg H. Development of a novel indwelling balloon applicator for optimizing light delivery in photodynamic therapy. Lasers Surg Med 2001;29:406-412.
130. Nyst HJ, van Veen RL, Tan IB, et al. Performance of a dedicated light delivery and dosimetry device for photodynamic therapy of nasopharyngeal carcinoma: phantom and volunteer experiments. Lasers Surg Med 2007;39:647-653.
131. Kostenich G, Orenstein A, Roitman L, Malik Z, Ehrenberg B. In vivo photodynamic therapy with the new near-IR absorbing water soluble photosensitizer lutetium texaphyrin and a high intensity pulsed light delivery system. J Photochem Photobiol B 1997;39:36-42.
132. Lapchak PA, Salgado KF, Chao CH, Zivin JA. Transcranial near-infrared light therapy improves motor function following embolic strokes in rabbits: an extended therapeutic window study using continuous and pulse frequency delivery modes. Neuroscience 2007;148:907-914.
133. Usuda J, Ichinose S, Ishizumi T, et al. Outcome of photodynamic therapy using NPe6 for bronchogenic carcinomas in central airways >1.0 cm in diameter. Clin Cancer Res 2010;16:2198-2204.
134. Cassidy CM, Tunney MM, Magee ND, et al. Drug and light delivery strategies for photodynamic antimicrobial chemotherapy (PACT) of pulmonary pathogens: a pilot study. Photodiagnosis Photodyn Ther 2011; 8:1-6.
135. Friedberg JS, Skema C, Burdick J, Yodh AG, Carr SR, Culver JP. A novel technique for light delivery through branched or bent anatomic structures. J Thorac Cardiovasc Surg 2003;126:1963-1967.
136. Wang LW, Li LB, Li ZS, Chen YK, Hetzel FW, Huang Z. Self-expandable metal stents and trans-stent light delivery: are metal stents and photodynamic therapy compatible? Lasers Surg Med 2008;40:651-659.
137. Yang L, Wei Y, Xing D, Chen Q. Increasing the efficiency of photodynamic therapy by improved light delivery and oxygen supply using an anticoagulant in a solid tumor model. Lasers Surg Med 2010;42:671-679.
138. Mitra S, Foster TH. Carbogen breathing significantly enhances the penetration of red light in murine tumours in vivo. Phys Med Biol 2004; 49:1891-1904.
139. Xiao Z, Dickey D, Owen RJ, Tulip J, Moore R. Interstitial photodynamic therapy of the canine prostate using intra-arterial administration of photosensitizer and computerized pulsed light delivery. J Urol 2007;178: 308-313.
140. Dickey D, Barajas O, Brown K, Tulip J, Moore RB. Radiance modelling using the P3 approximation. Phys Med Biol 1998;43:3559-3570.
141. Jankun J, Keck RW, Skrzypczak-Jankun E, Lilge L, Selman SH. Diverse optical characteristic of the prostate and light delivery system: implications for computer modelling of prostatic photodynamic therapy. BJU Int 2005;95:1237-1244.
142. Kostenich G, Babushkina T, Malik Z, Orenstein A. Photothermic treatment of pigmented B16 melanoma using a broadband pulsed light delivery system. Cancer Lett 2000;157:161-168.